Hafnium implanted in iron. I. Lattice location and annealing behaviour

1993 J. Phys.: Condens. Matter 5 2171

(http://iopscience.iop.org/0953-8984/5/14/014)

J. Phys.: Condens. Matter 5 (1993) 2171–2180. Printed in the UK

Hafnium implanted in iron: I. Lattice location and annealing behaviour

J M G J de Bakker, F Pleiter and P J M Smulders

Vakgroep Nucleaire Vaste Stof Fysica, Rijksuniversiteit Groningen, Nijenborgh 4, 9747 AG Groningen, The Netherlands

Received 24 August 1992, in final form 8 February 1993

Abstract. Perturbed angular correlation, Rutherford backscattering and channelling experiments were conducted to study the lattice location and annealing behaviour of 110 keV hafnium ions implanted into iron single crystals. It was found that a fraction of 11–25% of the implanted hafnium atoms are located at substitutional sites in an undisturbed environment, while about 50% are located at irregular lattice sites. The remaining fraction are located at or near regular lattice sites in a perturbed local environment. Trapping and detrapping of monovacancies by substitutional hafnium atoms at 200 and 250 K, respectively, as well as hafnium precipitation during annealing at 873 K was observed. The vacancy–hafnium binding energy was determined to be $E^{b}_{HfV_2} = 0.17(3)$ eV.

1. Introduction

Up until now, all studies on hafnium implanted in iron were focused on the determination of the magnitude of the magnetic hyperfine field of Hf or Ta in iron (Soares *et al* 1975, Herzog *et al* 1986, Cruz and Pleiter 1988). These hyperfine-interaction studies additionally showed that, despite the low solubility (Massalski 1986), at least 16% of the room-temperature implanted hafnium atoms are located at unique lattice sites with cubic symmetry, while the rest are distributed over irregular lattice sites. In order to study the interaction of nitrogen with hafnium in iron (see the subsequent paper, hereafter called II), we required more information on the system HfFe, especially on its behaviour as a function of annealing temperature. In this paper we present, therefore, perturbed angular correlation (PAC), Rutherford backscattering (RBS) and ion-channelling experiments performed on iron single crystals implanted with 110 keV hafnium.

2. Perturbed angular correlation experiments

2.1. Experimental details

Disc-shaped single crystals with a diameter of 12 mm and a thickness of 1 mm were cut by means of spark erosion from an iron slab produced by the strain-annealing method. The slab contained several single-crystalline areas of a few cm^2. The angle between the surface normal and the nearest (211) crystallographic direction was about

0953-8984/93/142171+10$07.50

5°, as determined by means of the x-ray back-reflection Greninger–Laue method. The purity of the iron was 99.98% (metallic impurities only). The crystal surfaces were prepared by mechanical and electrochemical polishing techniques.

The crystals were implanted with 110 keV radioactive ^{181}Hf ions to doses between 2×10^{12} and 2×10^{14} at. cm^{-2}. The crystal surface normal was usually tilted by 7° with respect to the incident beam direction. The implantations were carried out while the crystals were held at room temperature, apart from one crystal which was implanted at 77 K. The vacuum in the implantation chamber of the Groningen isotope separator was always better than 5×10^{-7} mbar.

Two crystals were annealed for about 20 min at step-wise increasing temperatures in the ranges 77–295 K and 293–973 K, respectively. The annealing treatments below room temperature were done by immersing the crystal in a mixture of diethyl ether and liquid nitrogen. The annealing treatments above room temperature were done in a vacuum of better than 1×10^{-8} mbar.

After the ^{181}Hf implantations and after each annealing treatment, the perturbed angular correlation of the 133–482 keV γ-ray cascade of the daughter nucleus ^{181}Ta was measured (Fransens *et al* 1991, Frauenfelder and Steffen 1968, Wichert and Recknagel 1986). We used a set-up with four detectors positioned at a distance of 40 mm from the source of radiation, at fixed relative angles of 180° and 90°. The detectors consisted each of a 44 mm⌀ × 30 mm BaF_2 crystal attached to a Philips XP2020Q photomultiplier, resulting in a time resolution of about 0.7 ns FWHM. We recorded four time spectra simultaneously, which were combined to form the four-spectrum conventional ratio $R(t)$ discussed by Arends *et al* (1980). The measuring temperatures were the same as the implantation temperatures. The crystals were magnetized in an external field of 0.17 T oriented in the plane of the detectors, at an angle of 45° with respect to the detector axes (Raghavan and Raghavan 1971). The magnetization direction was usually along a ⟨110⟩ crystallographic direction, parallel to the crystal surface. One measurement was performed with the field perpendicular to the detector plane in order to verify that the samples were completely magnetized.

2.2. *Results*

The ratio $R(t)$ and its Fourier transform $F(\omega)$ measured on an as-implanted crystal at room temperature are shown in figure 1. One observes a single well defined component with a magnetic interaction frequency $\omega_B = 3.80(3)$ Grad s^{-1}. We assign this frequency to substitutional ^{181}Hf atoms in a damage-free close environment (see section 5.1). Using the nuclear g factor $g_N = 1.30(1)$ (Ellis 1973) of the 482.0 keV state in ^{181}Ta, we calculate a value $|B_{hf}(RT)| = 61.0(5)$ T for the magnetic hyperfine field at substitutional tantalum in iron at room temperature. This value agrees within limits of error with the reported values $|B_{hf}(RT)| = 60.8(7)$ T (Cruz and Pleiter 1988) and 59.6(1.8) T (Soares *et al* 1975). The hyperfine field measured at 77 K has a value of $|B_{hf}(77\ K)| = 62.6(5)$ T, which is in agreement with the reported zero-temperature value $|B_{hf}(0\ K)| = 61.9(7)$ T (Cruz and Pleiter 1988).

We have determined the substitutional fraction f_S of ^{181}Hf implanted in Fe single crystals, by fitting the measured PAC spectra and taking into account the attenuation due to the finite time resolution and the finite solid angles subtended by the detectors. It turned out that f_S strongly decreases with implanted dose, the lowest value (11.0(4)%) being measured on a sample implanted with a dose of about 2×10^{14} at. cm^{-2}, the highest value (25.7(3)%) being measured on a sample implanted with a dose of about 2×10^{13} at. cm^{-2}. The value $f_S = 17(3)$%, observed

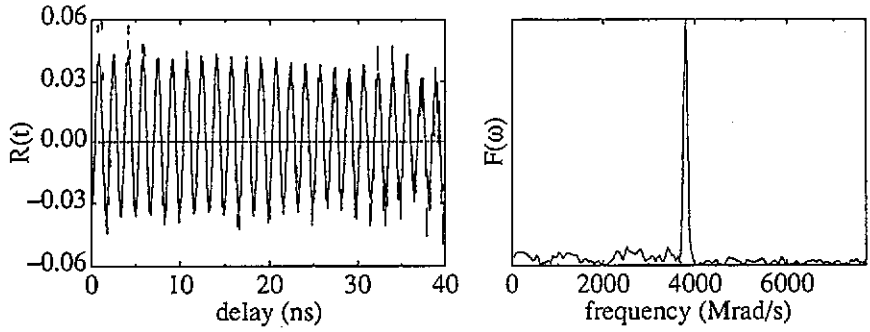

Figure 1. The ratio $R(t)$ and its Fourier transform $F(\omega)$ measured on an Fe single crystal implanted with 110 keV ^{181}Hf.

after implantation of 80 keV ^{181}Hf in an Fe foil to a dose of 2×10^{14} at. cm^{-2} (Soares *et al* 1975), is in line with our results. The reported value $f_s \simeq 45\%$ for an Fe(100) single crystal implanted with 110 keV ^{181}Hf to a dose of 2×10^{12} at. cm^{-2} (Cruz and Pleiter 1988) is very likely wrong.

A large fraction of the implanted probe nuclei is visible in the Fourier spectrum as a broad, ill defined distribution of interaction frequencies below ω_B. These atoms are located at non-unique lattice sites with low symmetry. They are probably subjected to combined electric and magnetic interactions of comparable strengths. The resulting interference of the multiple interaction frequencies causes the anisotropy to damp out within 10 ns (Pleiter *et al* 1977).

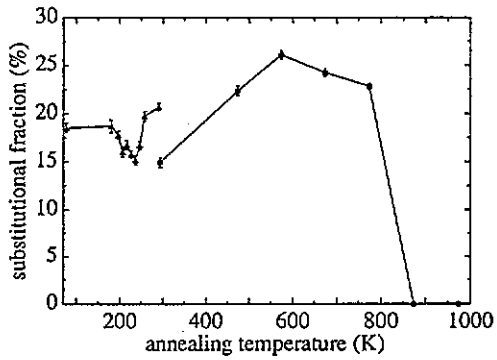

Figure 2. Substitutional fraction of ^{181}Hf implanted in Fe single crystals as a function of annealing temperature, as determined by means of PAC: (▲) $T_{impl} = T_{meas} = 77$ K; (●) $T_{impl} = T_{meas} = 295$ K.

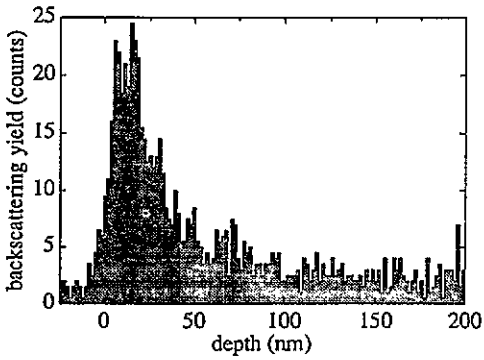

Figure 3. Depth profile of 110 keV Hf implanted in an Fe single crystal, measured by means of RBS.

In figure 2, the substitutional fraction is plotted as a function of annealing temperature for crystals implanted at 77 K and at 295 K. The step in f_S at about 295 K is most likely due to the difference in implanted dose. The decrease of f_S at 200 K indicates a loss of substitutional sites due to trapping of lattice defects which become mobile at this temperature. The increase of f_S at 250 K indicates detrapping of these lattice defects. Annealing at temperatures above room temperature results in

a monotonic increase of f_S up to a maximum at about 573 K. This reflects recovery of lattice damage which was introduced into the crystal during the Hf implantation. During annealing at 873 K the substitutional fraction f_S drops to zero. The PAC spectrum measured after this annealing treatment shows a very broad distribution of interaction frequencies extending from 0 to about 4 Grad s^{-1}.

3. Rutherford backscattering experiments

An Fe(211) single crystal was implanted at 293 K with 110 keV ^{180}Hf to a dose of 1×10^{14} at. cm^{-2}. RBS measurements were carried out with a 2.0 MeV $^4He^+$ beam from the Groningen Van de Graaff accelerator. The ions entered the sample in a pseudo-random crystallographic direction, approximately perpendicular to the surface. The backscattered helium ions were detected with silicon surface barrier detectors placed at exit angles of 10°, 40° and 70° with respect to the crystal surface.

The depth distribution measured on the as-implanted crystal is shown in figure 3. The profile resembles a Gaussian with an exponential tail extending up to at least 200 nm depth. The Gaussian is centred around a depth of 16 nm and has a width of about 10 nm FWHM. This is in reasonable agreement with the average range and straggling of $R = 18$ nm and $\Delta R = 6$ nm, respectively, obtained from a TRIM (Ziegler *et al* 1985) calculation for amorphous iron. The tail, however, is not reproduced in the TRIM calculation. This may be due to the fact that channelling effects have occurred during the implantation, in spite of the 7° tilt. A trajectory length of 200 nm for channelled Hf^+ ions is not unrealistically long, since e.g. particle ranges of more than 10 times the LSS projected range (Winterbon 1975) have been observed for 200 keV Au implanted in Cu under ⟨110⟩ axial alignment (Borders and Poate 1976). In view of the discussion in section 5.2, it is unlikely that the tail of the depth distribution is due to vacancy-assisted migration of the implanted Hf atoms. From the measured depth profile, we calculate a maximum Hf concentration of about 0.04 at. % for a dose of 1×10^{14} at. cm^{-2}. This corresponds to an average interatomic separation of about 14 lattice distances.

The crystal was annealed at 873 K for 20 min in a vacuum better than 1×10^{-7} mbar. The Hf depth profile measured after this treatment is practically identical to the one shown in figure 3.

4. Channelling experiments

4.1. Experimental details

An Fe(211) single crystal was implanted with 110 keV ^{180}Hf to a dose of 2.5×10^{14} at. cm^{-2}. Channelling experiments were carried out on the as-implanted crystal using a beam of 2.0 MeV $^4He^+$ ions. Energy spectra of ions scattered from the iron host lattice and the hafnium atoms were measured with three cooled silicon surface-barrier detectors. The detectors were placed at backscattering angles of ±165° and 135°, and had an average energy resolution of about 16 keV FWHM. During the measurements, the crystal was cooled to 163 K.

Angular yield curves around the ⟨100⟩, ⟨110⟩ and ⟨111⟩ crystallographic axes were constructed from spectra measured as a function of the tilt angle Ψ with respect to these directions. The energy spectra were summed over a region corresponding to a depth from 0 to 45 nm. All scans were taken in a plane making an angle θ

of roughly 15° with a {110} plane through the corresponding axis. Each scan was measured on a different spot on the crystal surface. The yield curves measured with the detector placed at −165° were used in the analysis of the Fe dips. The Hf yield curves obtained with all three detectors were averaged in order to improve statistics. Additionally, a constant background of less than 15% due to pile-up was subtracted.

4.2. Results

In figure 4, the experimental angular yield curves for the iron host and hafnium impurity are shown. The curves are normalized to the yield obtained at $\Psi = 5°$.

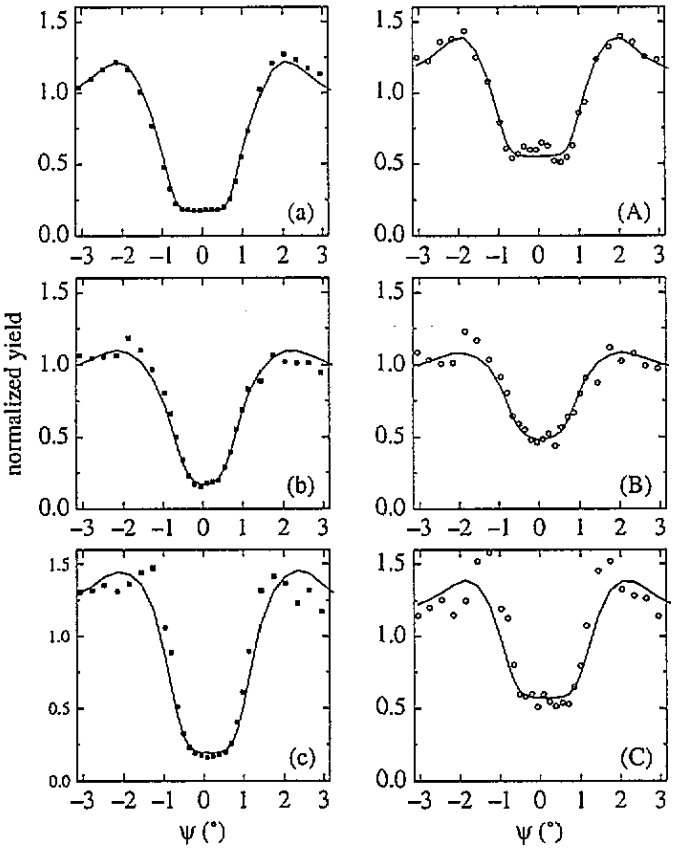

Figure 4. Normalized scattering yield as a function of the tilt angle Ψ with respect to the ⟨100⟩ (*a*, *A*), ⟨110⟩ (*b*, *B*) and ⟨111⟩ (*c*, *C*) axial directions, for 2 MeV helium ions backscattered from Fe (*a*, *b*, *c*) and Hf (*A*, *B*, *C*). Experimental points are indicated by squares and circles, simulated points are connected by full curves.

In all the yield curves, the measured minimum yield, $\chi_{min} \simeq 17\%$, of the host is significantly larger than the theoretically expected value for a perfect crystal (e.g. $\chi_{min,\{100\}} = 2\%$). The difference is partly due to the presence of a disordered surface (oxide) layer and partly to radiation damage introduced in the crystal during the hafnium implantation. However, we presume that the main contribution to the minimum yield arises from randomly displaced host atoms or dislocations, which were already present in the crystal before the Hf implantation. The analysing beam did not introduce significant

amounts of lattice damage. On the contrary, at the end of the angular scans we observed a decrease of χ_{min} by about 2.5% and 10% for the host and the impurity, respectively. This suggests that lattice disorder anneals out during the helium bombardment. The positive effect of post-irradiation on the substitutional fraction of implanted impurity atoms has been well documented (Meyer and Turos 1987).

The experimental host and impurity scans were simulated using the Monte Carlo program FLUX (Smulders and Boerma 1987). The smallest chi-square values were obtained assuming a Gaussian angular beam spread with standard deviation $\sigma = 0.1°$, 0.2° and 0.2° and an angle $\theta = 14°$, 17° and 16° for the ⟨100⟩, ⟨110⟩ and ⟨111⟩ scans, respectively. The simulated scans are shown as full curves in figure 4.

The large values of the angular beam spread cannot be solely due to the presence of a disordered surface layer, for $\sigma = 0.1°$ would require a surface layer thickness of at least 74 nm. This is much thicker than the average Hf depth. Moreover, such a thick layer would immediately be visible in the RBS energy spectrum measured in axial alignment, which is not the case. A possible explanation for the apparently extremely large beam spread could be that our single crystal is not perfect, but contains twinned or mosaic regions. This idea is supported by the fact that some regions of the crystal are of very bad quality as reflected by a measured minimum yield of 50% or more.

The lattice location of the implanted Hf atoms was determined by fitting simulated angular yield curves to the experimental curves for different assumed impurity lattice sites. In the simulations, we used the values of θ and σ given above. The best overall fits were obtained for a combination of Hf atoms located at regular lattice sites and randomly distributed impurity atoms. The results are shown in figure 4. The substitutional fractions derived from the fits amount to 48(3), 48(3) and 50(7)% for the ⟨100⟩, ⟨110⟩ and ⟨111⟩ directions, respectively. Due to the pure statistics of the Hf signal and the bad quality of the crystal, we cannot exclude the possibility that some of the substitutional Hf atoms are in fact slightly displaced from exact lattice sites.

5. Discussion

5.1. Lattice site location

By means of PAC and channelling experiments, we have obtained information about the lattice location of Hf ions implanted in Fe single crystals. The PAC results indicate that a fraction f_1 of the Hf atoms between 75 and 89%, depending on the implanted dose are located in a distorted environment. The rest, f_S, are located in a well defined surrounding with cubic symmetry. According to our channelling measurements, a fraction $f_2 \simeq 50\%$ of the implanted Hf atoms are found at random lattice sites while the rest are located at or slightly shifted from regular lattice sites. Combining the results of the two experiments, we conclude that a fraction $25 \leqslant f_3 \leqslant 39\%$, $f_3 = f_1 - f_2$, are located at or near regular lattice sites but do not contribute to the PAC signal.

One should be aware that PAC and channelling may yield quite different values of the so-called substitutional fraction (see, e.g., Meyer and Turos 1987, p 406). In a PAC experiment, f_S samples atoms in any cubic environment, including cubic defect structures. In a channelling experiment, f_S samples atoms at or near regular lattice sites, including impurity–vacancy clusters. In the following, we will use this difference in sampled properties to distinguish between the various lattice locations of the implanted Hf atoms, and discuss the pros and cons of some possible interpretations of the observed fractions.

$f_S \simeq 11$–25%. Taking the results from channelling and PAC measurements together, it is obvious that this fraction of Hf atoms is located at substitutional lattice sites. From the absence of an electric field gradient (EFG) we conclude that at least the nearest-neighbour shell has cubic symmetry and must, thus, be undistorted. In the following, we denote a substitutional Hf atom by HfV, where V stands for a vacancy.

$f_2 \simeq 50\%$. According to the equilibrium phase diagram, Hf is practically insoluble in α-iron (Massalski 1986). It is thus conceivable that this fraction of implanted Hf atoms has segregated and formed clusters or precipitates. Indeed, Hf atoms in clusters or (incoherent) precipitates are distributed at irregular lattice sites, and in channelling measurements, they would contribute a constant yield as a function of tilt angle. In PAC experiments, they would show up as being subjected to a variety of field gradients. As the mobility of Hf in Fe at the implantation temperatures is virtually zero, the segregation must have occurred during the cooling phase of the collision cascades (Meyer and Turos 1987). According to a TRIM.CAS (Biersack 1988) calculation, Hf doses higher than about 1×10^{12} at. cm^{-2} are required for the cascades to overlap. Because our samples are implanted with doses ranging from 2×10^{12} to 2.5×10^{14} at. cm^{-2}, segregation can indeed not be excluded. Only substitutional Hf atoms cause a well defined interaction frequency, whereas the other Hf atoms give rise to a broad distribution of frequencies. This is a strong indication that no large precipitates of any ordered phase are formed.

Hafnium is an oversized impurity in iron. Therefore, one may expect that Hf interacts with vacancies present in its near environment. In the damage cascades, vacancies are produced abundantly. These vacancies are spatially correlated with the position of the implanted atoms. Several vacancy–impurity complexes may form athermally during the cooling phase of the cascades and, above recovery stage III, by thermal activation of vacancy mobility (Meyer and Turos 1987). When extended vacancy clusters are formed around Hf atoms one expects large relaxations from regular lattice sites as well as strong electric field gradients. Thus, we may also attribute the fraction f_2 to Hf atoms that are associated with vacancies. Since the Hf–monovacancy cluster is unstable above 250 K (see section 5.2), such clusters must contain more than one vacancy.

$f_3 \simeq 25$–39%. According to our channelling measurements these atoms are not located in Hf clusters or (incoherent) precipitates. For the same reason, these atoms are not located in large vacancy clusters. However, they may be associated with small vacancy clusters consisting of one or two vacancies. Indeed, the very small relaxation of a substitutional solute atom associated with one or two trapped vacancies may not be observable by channelling. This has been shown, e.g., in the combined PAC and channelling measurements on the system InCu: In–vacancy and In–divacancy complexes were not observed by the channelling method, while they were easily detectable by the PAC technique because of the large local EFG (Swanson *et al* 1984). Thus one might expect that the fraction f_3 consists of atoms associated with one or two vacancies. Since Hf–monovacancy clusters (HfV_2) are thermodynamically unstable at room temperature (see section 5.2), we are left with Hf–divacancy complexes (HfV_3) to explain fraction f_3.

Another possible explanation for the fraction f_3 which we will consider here is trapping of interstitial impurity atoms such as N, C or O. We do not have data on the concentration of these impurities in the used Fe(211) single crystals. However, we have also implanted an Fe(100) crystal of 3*N* purity acquired from Materials

Research Corporation. The carbon and oxygen concentrations determined by means of charged particle activation analysis are 1 ppm and 35 ppm respectively; the nitrogen concentration is unknown. With such crystals, Metz and Niesen (1989) have observed an anomalous behaviour in NMR-ON experiments as compared to crystals with higher purity, which they tentatively attributed to the association of oxygen with the implanted ^{131}I probe nuclei. We have observed a substitutional fraction of $f_S = 12.2(5)\%$ at an implanted dose of 3×10^{14} at. cm^{-2}, which is comparable to the results obtained with the Fe(211) crystals. Nitrogen, oxygen and carbon interstitials are immobile in iron at 77 K and hardly mobile at room temperature (Fromm and Gebhardt 1976). If these impurities are indeed trapped, they must have been mobilized during the energetic damage cascades produced by the impinging Hf ions.

5.2. Interaction with monovacancies

The low-temperature isochronal annealing experiments on ^{181}Hf implanted Fe show defect trapping and detrapping near 200 and 250 K, respectively. In PAC experiments performed on the system ^{111}InFe, a dip in the substitutional fraction has been observed, which is very similar to the one shown in figure 2, and which has been associated with freely migrating vacancies (Pleiter *et al* 1981). This idea is supported by the results of a series of measurements on positron lifetime (Hautojärvi 1983) and muon spin rotation (Möslang *et al* 1983, Weidinger 1984) which have clearly shown that monovacancies in iron become mobile near 200 K. This temperature corresponds to defect recovery stage III, according to the one-interstitial model (Schilling *et al* 1975).

Weidinger has proposed two possible explanations for the disappearance of the frequency associated with a vacancy–impurity pair a few tens of Kelvin above the trapping temperature in his muon spin rotation experiments on the systems CoFe, NiFe, SiFe, CuFe and AuFe: (i) break-up of the vacancy–impurity pair or (ii) migration of the vacancy–impurity pair (no break-up) and formation of vacancy–impurity clusters. His experiments could not definitely distinguish between these two possibilities. However, on the basis of our PAC measurements and considering the similarity between the annealing behaviour of the HfFe system and the systems studied by Weidinger, we may propose option (i) as the proper explanation, because option (ii) would not lead to the observed increase of f_S.

An estimate of the vacancy–hafnium binding energy, $E^{b}_{HfV_2}$, may be obtained in the following way. Let T_1 be the temperature at which half of the impurities have trapped a vacancy. This requires on the average n_1 jumps:

$$n_1 = \Delta t \nu_0 \exp(-E^{m}_{V}/k_B T_1) \tag{1}$$

where E^{m}_{V} is the vacancy migration energy, Δt is the annealing time, and ν_0 is the monovacancy jump frequency. For the vacancy–impurity to break up, n_2 jumps of the vacancy away from the impurity are required:

$$n_2 = \Delta t \nu_0 \exp(-E^{d}_{HfV_2}/k_B T_2) \tag{2}$$

where T_2 is the temperature at which the substitutional fraction has recovered to half of the initial value and $E^{d}_{HfV_2}$ is the vacancy–solute dissociation energy given by

$$E^{d}_{HfV_2} = E^{b}_{HfV_2} + E^{m}_{V}. \tag{3}$$

Combining equations (1), (2) and (3) yields

$$E^{b}_{HfV_2} = E^{m}_{V}(T_2 - T_1)/T_1 + k_B T_2 \ln(n_1/n_2). \tag{4}$$

We have assumed that the effective jump frequencies for free vacancies and solute-associated vacancies do not differ appreciably. We take $5 \leqslant n_1 \leqslant 21$ (Van der Kolk *et al* 1985), and assume a single-step detrapping process with $n_2 = \ln 2$. If we take the calculated value 0.68 eV for the monovacancy migration energy (Beeler and Johnson 1967), and the observed temperatures $T_1 = 200(5)$ K and $T_2 = 250(5)$ K, we finally obtain $E^{b}_{HfV_2} = 0.17(3)$ eV. Similar values have been obtained for other impurity–vacancy pairs in iron (Möslang *et al* 1983).

5.3. High-temperature behaviour

Bowen and Leak (1970) have determined the tracer diffusion coefficient of Hf in stabilized α-Fe in the temperature range from 1371 to 1657 K. They found

$$D = D_0 \exp(-E/k_B T) \tag{5}$$

with the pre-exponential factor $D_0 = 1.31(^{+94}_{-55}) \times 10^{-4}$ m^2 s^{-1} and activation energy $E = 3.01(17)$ eV. From the Einstein equation for random-walk diffusion in an isotropic crystal (Peterson 1978)

$$\langle R^2 \rangle = 6Dt \tag{6}$$

we can calculate the root-mean-square displacement of Hf in Fe after annealing for $t = 1200$ s at 873 K. Extrapolation of relation (5) to $T = 873$ K yields $D = 5 \times 10^{-22}$ m^2 s^{-1} and, inserting this into equation (6), we obtain $\langle R^2 \rangle^{1/2} \simeq 2$ nm. This distance is too small for massive diffusion towards the crystal surface. Though the values given by Bowen and Leak are thought to be not very reliable (Oikawa 1983), they are in agreement with the results from our RBS measurements. Indeed we did not observe long-range diffusion after annealing at 873 K. However, on the basis of the calculated root-mean-square displacement and our RBS measurements, we cannot exclude formation of hafnium clusters or precipitates. The occurrence of precipitation is not unlikely, given the very low solubility limit of Hf in Fe. We conclude that precipitation is a possible explanation for the sudden drop in f_S observed in the system ^{181}HfFe by means of PAC after annealing at 873 K.

One might attribute the reduction of f_S to the trapping of interstitially migrating impurities such as O, N or C. These impurities are highly mobile in Fe at much lower temperatures than 873 K (Fromm and Gebhardt 1976). Thus, their appearance in solution and diffusion towards the probe nuclei must be preceded by dissociation of solute or solute–vacancy clusters. However, carbon–vacancy (Takaki *et al* 1983) and nitrogen–vacancy (Swanson *et al* 1985) clusters break up at already 560 K and 650 K, respectively. At these temperatures f_S does not change significantly. Furthermore, nitrogen-associated hafnium dissociates at 773 K (see II). It is therefore unlikely that formation of Hf–N and Hf–C complexes is the cause of the decrease of f_S.

6. Conclusions

By means of perturbed angular correlation, Rutherford backscattering and channelling experiments, we have investigated the lattice site location and annealing behaviour of 110 keV hafnium implanted into iron single crystals. It was found that a fraction of 11–25% of the implanted hafnium atoms are located at substitutional sites in an undisturbed environment, while about 50% are located at random lattice sites.

The remaining atoms are located at or near regular lattice sites in a perturbed local environment. Trapping and detrapping of monovacancies by substitutional hafnium atoms at 200 and 250 K, respectively, as well as hafnium precipitation during annealing at 873 K was observed. The binding energy of a vacancy–hafnium pair was determined to be $E^{b}_{HfV_2} = 0.17(3)$ eV.

Acknowledgments

This work was performed as a part of the research programme of the Stichting voor Fundamenteel Onderzoek der Materie (FOM), with financial support from the Nederlandse Organisatie voor Wetenschappelijk Onderzoek (NWO).

References

Arends A R, Hohenemser C, Pleiter F, De Waard H, Chow L and Suter R M 1980 *Hyperfine Interact.* **8** 191

Beeler J R and Johnson R A 1967 *Phys. Rev.* **156** 667

Biersack J P 1988 *TC(1990) vers. 3.5* PC version of FORTRAN Monte Carlo program TRIM.CAS

Borders J A and Poate J M 1976 *Phys. Rev.* B **13** 969

Bowen A W and Leak F M 1970 *Metall. Trans.* **1** 1695

Cruz M M and Pleiter F 1988 *Hyperfine Interact.* **39** 389

Ellis Y A 1973 *Nucl. Data Sheets* **9** 319

Fransens J R, Abd El Keriem M S and Pleiter F 1991 *J. Phys.: Condens. Matter* **3** 9871

Frauenfelder H and Steffen R M 1968 *Alpha-, Beta-, and Gamma-Ray Spectroscopy* vol 2, ed K Siegbahn (Amsterdam: North-Holland) ch XIXA

Fromm E and Gebhardt E 1976 *Gase und Kohlenstoff in Metallen* (Berlin: Springer)

Hautojärvi P 1983 *Hyperfine Interact.* **15/16** 357

Herzog P, Dämmrich U, Freitag K, Herrmann C-D, Schlösser K and Soares J C 1986 *Z. Phys.* B **63** 241

Massalski T B 1986 *Binary Alloy Phase Diagrams* vol 1 (Metals Park, OH: American Society for Metals)

Metz A and Niesen L 1989 *Phys. Rev.* B **39** 2029

Meyer O and Turos A 1987 *Mater. Sci. Rep.* **2** 371

Möslang A, Albert E, Recknagel E and Weidinger A 1983 *Hyperfine Interact.* **15/16** 409

Oikawa H 1983 *Technol. Rep. Tohoku Univ.* **48** 7

Peterson N L 1978 *Properties of Atomic Defects in Metals* ed N L Peterson and R W Siegel (Amsterdam: North-Holland) p 3

Pleiter F, Arends A R and Devare H G 1977 *Hyperfine Interact.* **3** 87

Pleiter F, Hohenemser C and Arends A R 1981 *Hyperfine Interact.* **10** 691

Raghavan R S and Raghavan P 1971 *Nucl. Instrum. Methods* **92** 435

Schilling W, Ehrhart P and Sonnenberg K 1975 *Fundamental Aspects of Radiation Damage in Metals (CONF-7510006-P1, Gatlinburg, TN)* ed M T Robinson and F W Young Jr p 470

Smulders P J M and Boerma D O 1987 *Nucl. Instrum. Methods* B **29** 471

Soares J C, Krien K and Freitag K 1975 *Hyperfine Interact.* **1** 45

Swanson M L, Howe L M, Jackman J A, Jackman T E, Griffiths K and Quenneville A F 1985 *Nucl. Instrum. Methods* B **7/8** 85

Swanson M L, Howe L M, Quenneville A F, Wichert Th and Deicher M 1984 *J. Phys. F: Met. Phys.* **14** 1603

Takaki S, Fuss J, Kugler H, Dedek U and Schultz H 1983 *Radiat. Eff.* **79** 87

Van der Kolk G J, Post K, Van Veen A, Pleiter F and De Hosson J Th M 1985 *Radiat. Eff.* **84** 131

Weidinger A 1984 *Hyperfine Interact.* **17–19** 153

Wichert Th and Recknagel E 1986 *Microscopic Methods in Metals (Topics in Current Physics 40)* ed U Gonser (Berlin: Springer) p 317

Winterbon K B 1975 *Ion Implantation Range and Energy Deposition Distributions* vol 2 (New York: Plenum)

Ziegler J F, Biersack J P and Littmark U 1985 *The Stopping and Range of Ions in Solids* (New York: Pergamon)